

Quinonoid Oligothiophenes as Electron-Donor and Electron-Acceptor Materials. A Spectroelectrochemical and Theoretical Study

Juan Casado,^{†,‡} Larry L. Miller,^{*,‡} Kent R. Mann,[‡] Ted M. Pappenfus,[‡]
Hiroyuki Higuchi,[§] Enrique Ortí,^{*,||} Begoña Milián,^{||} Rosendo Pou-Américo,^{||}
Víctor Hernández,[†] and Juan T. López Navarrete^{*,†}

Contribution from the Departamento de Química Física, Facultad de Ciencias, Universidad de Málaga, 29071-Málaga, Spain, Department of Chemistry, Faculty of Science, Toyama University, 3190 Gofuku, Toyama, Japan, Institut de Ciència Molecular, Universitat de València, 46100-Burjassot (València), Spain, and Department of Chemistry, University of Minnesota, Minneapolis, Minnesota 55455

Received June 4, 2002

Abstract: Two quinonoid bis(dicyanomethylene) oligothiophenes, terthiophene and quaterthiophene analogues of TCNQ, have been investigated by spectroelectrochemical experiments and density functional theory calculations. Electrochemical data show that the molecules can be both reduced and oxidized at relatively low potentials, and that the quaterthiophene derivative forms four stable redox species, the dianion, neutral, cation radical, and dication. The neutral oligomers are characterized by a strong electronic absorption in the red or near-infrared region and can be viewed as structural and electronic analogues of aromatic oligothiophenes in the dication or bipolaron state. Upon reduction, dianions, not anion radicals, are formed which absorb in the visible region. The theoretical calculations show that the dianions have aromatic oligothiophene moieties with two anionic dicyanomethylene groups. The transition from a quinonoid to an aromatic structure is fully supported by UV–vis–near-IR and vibrational spectroscopic data. Oxidation, generating cation radicals and dications, occurs at rather low potentials similar to those reported for oligothiophenes. The electronic spectra of these cations are understood from the calculations, which suggest that the oxidized species are stabilized by the partial aromatization of the oligothiophene backbone. IR spectra of the species, especially the CN stretching frequencies, confirm the structural conclusions and allow comparison with TCNQ and the TCNQ dianion.

Introduction

Oligothiophenes have assumed an important place in materials chemistry, and in recent years there have been many studies of the structure and properties of these compounds. A particular attribute of importance for their application is their ease of oxidation. Cation radicals and higher oxidation states are formed at rather low potentials, and these species have considerable stability. In contrast, oligothiophenes are quite difficult to reduce and do not form stable anion radicals. This situation has been addressed by the synthesis of several quinonoid oligothiophenes,^{1–3} such as the dihexylbis(dicyanomethylene)quaterthiophene H4Th4CN4 (Figure 1). This compound, which is an

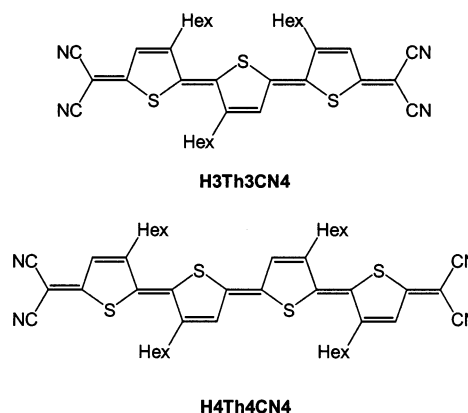


Figure 1. Chemical structures of the oligothiophenes studied in this work.

analogue of TCNQ, was shown to be reduced electrochemically at rather positive potentials. In the present paper we report further studies of this compound and its quinonoid terthiophene analogue H3Th3CN4.

There are many suggested applications of oligothiophenes including their use in thin-film field effect transistors (FETs).^{4,5} Our idea is that quinonoid oligothiophenes are interesting for

* Address correspondence to these authors. E-mail: (J.T.L.N.) teodomiro@uma.es; (L.L.M.) lmiller@chem.umn.edu; (E.O.) enrique.orti@uv.es.

[†] Universidad de Málaga.

[‡] University of Minnesota.

[§] Toyama University.

^{||} Universitat de València.

(1) Yui, K.; Aso, Y.; Otsubo, T.; Ogura, F. *Bull. Chem. Soc. Jpn.* **1989**, *62*, 1539.

(2) (a) Higuchi, H.; Yoshida, S.; Uraki, Y.; Ojima, J. *Bull. Chem. Soc. Jpn.* **1998**, *71*, 2229. (b) Hernández, V.; Losada, C.; Casado, J.; Higuchi, H.; López-Navarrete, J. T. *J. Phys. Chem. A* **2000**, *104*, 661.

(3) Higuchi, H.; Nakayama, T.; Koyama, H.; Ojima, J.; Wada, T.; Sasabe, H. *Bull. Chem. Soc. Jpn.* **1995**, *68*, 2363.

FET applications because they might be both oxidizable and reducible. Thus, one might devise ambipolar FETs using a compound such as H4Th4CN4 that could support the introduction of either negative or positive charges, and in this way act as both a p-type and n-type semiconductor when properly polarized. Recently, this idea has been tested using a quinonoid terthiophene, Bu2Th3CN4.⁶ Vapor- or solution-deposited films gave n-channel FETs with mobilities as high as 0.005 cm²/(V s). These mobilities are within an order of magnitude of the highest field effect mobilities observed for n-channel organic materials. No evidence was obtained for p-type conductivity, but we suggest that this might be observed with more extended quinonoid oligothiophenes. On the basis of the work reported here, such compounds will have lower oxidation potentials.

Whether these quinonoid molecules find FET applications depends on developing an understanding of their chemistry, and there is, indeed, a lot to learn. Here, we elucidate the structure, redox properties, and spectroscopy of H4Th4CN4 and its terthiophene analogue H3Th3CN4. Using a combination of spectroelectrochemistry and theoretical calculations, we document and explain several aspects of H4Th4CN4 chemistry such as its ease of oxidation, the stability of its cation radical and dication, the formation of the dianion (not the anion radical) upon reduction, and the electronic spectra of its four different oxidation states and their relationship to ordinary oligothiophenes and to TCNQ. In a complementary paper,⁷ we have studied a similar quinonoid terthiophene, Bu2Th3CN4, and the related α,α' -dinitroterthiophene structure with an emphasis on their redox chemistry and crystal structures. Both compounds crystallize in face-to-face π -stacks rather than the usual herringbone structures found for oligothiophenes. Without the evidence from theoretical calculations, such as those reported here, similar structural conclusions were reached.

Experimental and Computational Details

The synthesis and purification of H3Th3CN4 and H4Th4CN4 are described elsewhere.³ Cyclic voltammetry and spectroelectrochemical measurements were carried out in a 0.1 M tetrabutylammonium tetrafluoroborate (TBABF₄)/CH₂Cl₂ solution. H3Th3CN4 and H4Th4CN4 were prepared in a 0.053 M concentration in all the experiments. Electrochemical measurements were carried out using a Ag/AgCl electrode as reference electrode. A glassy carbon electrode and a platinum electrode were used as working and auxiliary electrodes, respectively. Electronic spectra in the vis-near-IR region (400–2000 nm) were obtained with a Perkin-Elmer Lambda 19 spectrometer. Spectra in the IR region (4000–1000 cm⁻¹) were obtained with a Nicolet 550 IR spectrometer equipped with an MCD detector. Electrolyses were controlled by a BAS-100 bulk electrolysis program.

All the theoretical calculations including geometry optimizations, electronic excitation energies, and IR spectra were carried out at the

DFT level using Becke's three-parameter B3LYP exchange-correlation functional⁸ and the 6-31G** basis set.⁹ Radical anions and radical cations were treated as open-shell systems and were computed using spin-unrestricted UB3LYP wave functions. The maximum value obtained for S^2 was 0.76, very close to the value of 0.75 theoretically required for a doublet, showing that spin contamination is almost absent. The calculated harmonic vibrational frequencies were scaled by a factor of 0.96 as recommended by Scott and Radom.¹⁰ All quoted vibrational data are thus scaled values. Vertical electronic excitation energies were computed by using the time-dependent density functional theory (TDDFT).^{11–14} The 20 lowest-energy excited states were calculated for all the molecular species. The computational cost of TDDFT is roughly comparable to that of single-excitation theories based on a Hartree–Fock (HF) ground state, such as single-excitation configuration interaction (CIS). Numerical applications reported so far indicate that TDDFT employing current exchange-correlation functionals performs significantly better than HF-based single-excitation theories for the low-lying valence excited states of closed-shell^{15,16} and open-shell¹⁷ molecules.^{18,19} All the calculations were performed using the A.7 revision of the Gaussian 98 program package²⁰ running on SGI Origin 2000 computers and IBM RS/6000 workstations.

Results and Discussion

Structure Calculations on Neutral Compounds. The molecular geometries of H3Th3CN4 and H4Th4CN4 were optimized assuming fully planar C_s and C_{2h} structures, respectively, in which the oligothiophene chains are in all-anti arrangements and the hexyl chains lie in the plane of the molecule in fully staggered conformations.

Figure 2 displays the optimized B3LYP/6-31G** bond lengths calculated for the carbon skeleton of H3Th3CN4 and H4Th4CN4. The shortest carbon–carbon (CC) distances correspond to the C_β – C_β bonds of the thiophene rings (~ 1.37 Å), to the inter-ring bonds (1.38–1.39 Å), and to the terminal bonds connecting the oligothiophene unit to the dicyanomethylene groups (1.39 Å). The thiophene C_α – C_β bonds are longer and have lengths of 1.425–1.459 Å for the trimer and 1.417–1.455 Å for the tetramer. These data are in good agreement with the X-ray structure recently obtained for the bis(dicyanomethylene)-terthiophene Bu2Th3CN4^{6,7} and show that the ground-state

(8) Becke, A. D. *J. Chem. Phys.* **1993**, *98*, 1372.

(9) Francl, M. M.; Pietro, W. J.; Hehre, W. J.; Binkley, J. S.; Gordon, M. S.; Defrees, D. J.; Pople, J. A. *J. Chem. Phys.* **1982**, *77*, 3654.

(10) Scott, A. P.; Radom, L. *J. Phys. Chem.* **1996**, *100*, 16502.

(11) Runge, E.; Gross, E. K. U. *Phys. Rev. Lett.* **1984**, *52*, 997.

(12) Gross, E. K. U.; Kohn, W. *Adv. Quantum Chem.* **1990**, *21*, 255.

(13) Gross, E. K. U.; Ullrich, C. A.; Gossmann, U. J. In *Density Functional Theory*; Gross, E. K. U., Driessler, R. M., Eds.; Plenum Press: New York, 1995; p 149.

(14) Casida, M. E. In *Recent Advances in Density Functional Methods, Part I*; Chong, D. P., Ed.; World Scientific: Singapore, 1995; p 155.

(15) Wiberg, K. B.; Stratmann, R. E.; Frisch, M. J. *J. Chem. Phys. Lett.* **1998**, *297*, 60. Stratmann, R. E.; Scuseria, G. E.; Frisch, M. J. *J. Chem. Phys.* **1998**, *109*, 8218.

(16) Hsu, C.-P.; Hirata, S.; Head-Gordon, M. *J. Phys. Chem. A* **2001**, *105*, 451.

(17) Hirata, S.; Lee, T. J.; Head-Gordon, M. *J. Chem. Phys.* **1999**, *111*, 8904.

(18) Koch, W.; Holthausen, M. C. *A Chemist's Guide to Density Functional Theory*; Wiley-VCH: Weinheim, Germany, 2000.

(19) Fabian, J. *Theor. Chem. Acc.* **2001**, *106*, 199.

(20) Frisch, M. J.; Trucks, G. W.; Schlegel, H. B.; Scuseria, G. E.; Robb, M. A.; Cheeseman, J. R.; Zakrzewski, V. G.; Montgomery, J. A.; Stratman, R. E.; Burant, J. C.; Dapprich, S.; Millam, J. M.; Daniels, A. D.; Kudin, K. N.; Strain, M. C.; Farkas, O.; Tomasi, J.; Barone, V.; Cossi, M.; Cammi, R.; Mennucci, B.; Pomelli, C.; Adamo, C.; Clifford, S.; Ochterski, J.; Petersson, G. A.; Ayala, P. Y.; Cui, Q.; Morokuma, K.; Malick, D. K.; Rabuck, A. D.; Raghavachari, K.; Foresman, J. B.; Cioslowski, J.; Ortiz, J. V.; Baboul, A. G.; Stefanov, B. B.; Liu, G.; Liashenko, A.; Piskorz, P.; Komaromi, I.; Gomperts, R.; Martin, R. L.; Fox, D. J.; Keith, T.; Al-Laham, M. A.; Peng, C. Y.; Nanayakkara, A.; Gonzalez, C.; Challacombe, M.; Gill, P. M. W.; Johnson, B.; Chen, W.; Wong, M. W.; Andres, J. L.; Head-Gordon, M.; Replogle, E. S.; Pople, J. A. *Gaussian 98, Revision A.7*; Gaussian, Inc.: Pittsburgh, PA, 1998.

(4) For a review of organic thin film FETs, see: Dimitrakopoulos, C. D.; Malenfant, P. R. L. *Adv. Mater.* **2002**, *14*, 99.

(5) Katz, H. E. *J. Mater. Chem.* **1997**, *7*, 369. Horowitz, G.; Garnier, F.; Yassar, A.; Hajlaoui, R.; Kouki, F. *Adv. Mater.* **1996**, *8*, 52. Garnier, F. *Acc. Chem. Res.* **1999**, *32*, 209. Garnier, F.; Yassar, A.; Hajlaoui, R.; Deloffre, F.; Servet, B.; Ries, S.; Alnot, P. *J. Am. Chem. Soc.* **1993**, *115*, 8716. Nelson, S. F.; Lin, Y. Y.; Gundlach, D. J.; Jackson, T. N. *Appl. Phys. Lett.* **1998**, *72*, 1854. Hong, X. M.; Katz, H. E.; Lovinger, A. J.; Wang, B.; Raghavachari, K. *Chem. Mater.* **2001**, *13*, 4686. Li, X. C.; Sirringhaus, H.; Garnier, F.; Holmes, A. B.; Morattie, S. C.; Feeder, N.; Clegg, W.; Teat, S. J.; Friend, R. H. *J. Am. Chem. Soc.* **1998**, *120*, 2206. Lanquandunum, J. G.; Katz, H. E.; Lovinger, A. J.; Dodabalapur, A. *Adv. Mater.* **1997**, *9*, 36. Katz, H. E. *J. Mater. Chem.* **1997**, *18*, 87.

(6) Pappenfus, T. M.; Chesterfield, R. J.; Frisbie, C. D.; Mann, K. R.; Casado, J.; Raff, J. D.; Miller, L. L. *J. Am. Chem. Soc.* **2002**, *124*, 4184.

(7) Pappenfus, T. M.; Raff, J. D.; Hukkanen, E. J.; Burney, J. R.; Casado, J.; Drew, S. M.; Miller, L. L.; Mann, K. R. *J. Org. Chem.* **2002**, *67*, 6015.

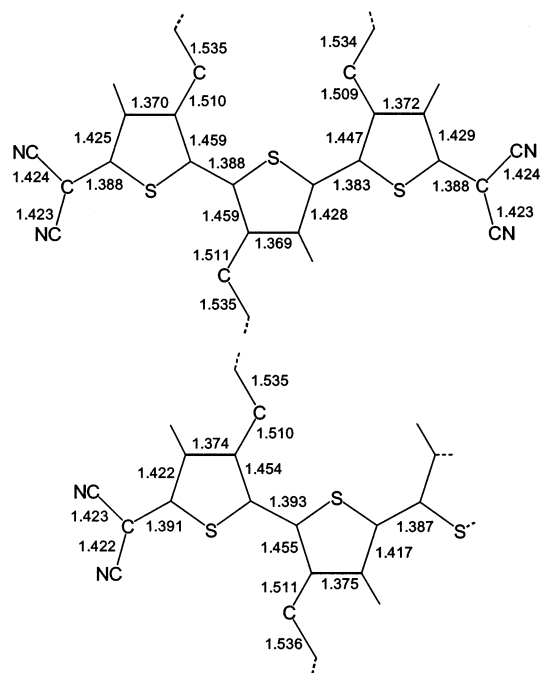


Figure 2. B3LYP/6-31G**-optimized bond lengths (Å) for H3Th3CN4 (top, C_s symmetry) and H4Th4CN4 (bottom, C_{2h} symmetry).

equilibrium geometries of H3Th3CN4 and H4Th4CN4 correspond to heteroquinonoid structures. The oligothiophene backbones exhibit a reversal of the single–double CC bond alternation pattern with respect to that observed for aromatic oligothiophenes, for which the C_β – C_β bonds and the inter-ring C_α – C_α' bonds are longer than the C_α – C_β bonds.

It is generally accepted that aromatic oligothiophenes display a quinonoid structure in their dication or bipolaron state. The quinonoid structures here obtained for H3Th3CN4 and H4Th4CN4 are in fact similar to those predicted theoretically for the dications of aromatic oligothiophenes.²¹ In this sense, H3Th3CN4 and H4Th4CN4 can be viewed as structural analogues of dicationic oligothiophenes.

The double-bond character of the inter-ring bonds in H3Th3CN4 and H4Th4CN4 precludes the internal rotation around these bonds, thereby imposing a planar structure, and renders these molecules with a more rigid structure than that found for aromatic oligothiophenes. The structure of the tetramer, with hexyl chains replaced by methyl groups to simulate steric effects, was in fact optimized starting from a nonplanar C_2 geometry, and no significant deviation from planarity was found. The alkyl chains induce a degree of asymmetry in the CC conjugation path. The C_α – C_β bonds to which they are linked are about 0.03 Å longer than their counterparts in the thiophene rings because of the additional steric contacts (C---S, 3.03 Å; H---S, 2.68 Å) they introduce in the interannular regions.

The net atomic charges calculated using Mulliken population analysis reveal that electron density is transferred from the oligothiophene backbone to the electron-withdrawing dicyanomethylene groups. For H3Th3CN4, each C(CN)₂ group bears a negative charge of –0.31e which is obtained from both the outer rings (+0.22e) and the central ring (+0.18e). For

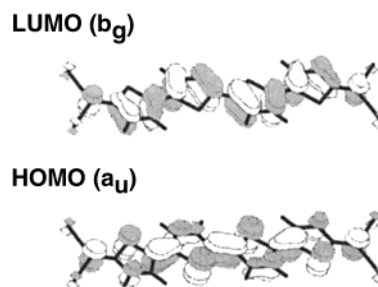


Figure 3. Electronic density contours (0.03 e/bohr³) calculated for the HOMO and LUMO of H4Th4CN4 at the B3LYP/6-31G** level. Hexyl chains are not depicted.

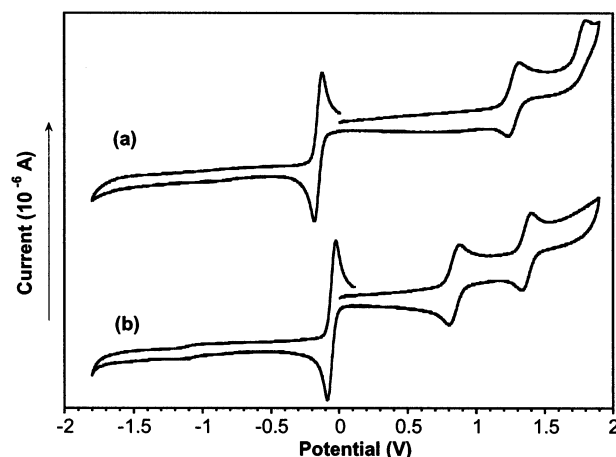


Figure 4. Cyclic voltammograms of H3Th3CN4 (a) and H4Th4CN4 (b) in 0.1 M TBABF₄/CH₂Cl₂ (scan rate 100 mV s⁻¹, reference Ag/AgCl).

H4Th4CN4, net charges of –0.33e, +0.20e, and +0.13e are calculated for the C(CN)₂ groups, outer thiophene rings, and central thiophene rings, respectively.

Figure 3 shows the atomic orbital composition calculated for the highest occupied molecular orbital (HOMO) and the lowest unoccupied molecular orbital (LUMO) of H4Th4CN4.

Both orbitals are of π nature, as expected, but their topologies are reversed with respect to those observed for aromatic oligothiophenes.²² This reversal is due to the quinonoid structure of the oligothiophene backbone and determines that the HOMO–LUMO energy gaps calculated at the B3LYP/6-31G** level for H3Th3CN4 (1.72 eV) and H4Th4CN4 (1.35 eV) are much smaller than those found for aromatic terthiophene (3.45 eV) and quaterthiophene (3.03 eV) at the same computational level.²³ The small HOMO–LUMO gaps predicted for H3Th3CN4 and H4Th4CN4 explain, in a first approach, the low-energy vis–near-IR absorptions of these molecules.

Electrochemical Properties. The cyclic voltammograms recorded for H3Th3CN4 and H4Th4CN4 in CH₂Cl₂ solution are shown in Figure 4.

Both oligomers exhibit a reversible two-electron reduction wave at $E^{\circ'}$ = –0.153 and –0.086 V, respectively. This wave corresponds to the reduction of both dicyanomethylene groups and directly leads to the formation of the dianion. The less negative $E^{\circ'}$ of the tetramer compared to the trimer is due to the mitigation of the on-site Coulomb repulsions between the

(21) (a) Alemán, C.; Juliá, L. J. *Phys. Chem.* **1996**, *100*, 14661. (b) Irle, S.; Lischka, H. J. *Chem. Phys.* **1997**, *107*, 3021. (c) Moro, G.; Scalmani, G.; Cossentino, U.; Pitea, D. *Synth. Met.* **1998**, *92*, 69.

(22) Lögdlund, M.; Dannetun, P.; Fredriksson, C.; Salaneck, W. R.; Brédas, J.-L. *Phys. Rev. B* **1996**, *53*, 16327.

(23) Aromatic terthiophene (C_{2v}) and quaterthiophene (C_{2h}) were optimized in a fully planar all-anti conformation at the B3LYP/6-31G** level.

negative charges as the size of the oligomer increases. Previous electrochemical studies on dicyanomethylene-substituted bithiophene indicated two sequential one-electron reductions as also observed for TCNQ.^{2,3} The difference between the two reduction potentials recorded for the bithienoquinonoid derivatives (about 0.2 V) was however significantly smaller than that measured for TCNQ (0.72 V), suggesting a decrease of the Coulomb repulsion in the dianion state of the former. As expected, the Coulomb repulsion is even smaller for the larger oligomers studied here, and the single two-electron reduction peak indicates that the anion radical is less stable than the dianion or at least of comparable stability so that the two processes occur under the same reduction wave.

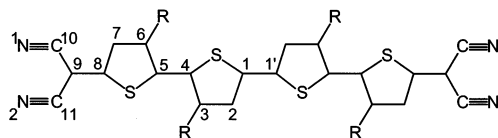
In addition to the two-electron reduction, H3Th3CN4 and H4Th4CN4 exhibit two one-electron oxidations. The first oxidation process is reversible and occurs at $E^{\circ} = 0.83$ V for H4Th4CN4 and at $E^{\circ} = 1.27$ V for H3Th3CN4. The second oxidation is recorded at $E^{\circ} = 1.37$ V for the tetramer and is also reversible. This is the first report to our knowledge of a stable dication from a quinonoid oligothiophene. As discussed above, the oligothiophene backbones in H3Th3CN4 and H4Th4CN4 are expected to be electron-deficient due to the electron-withdrawing dicyanomethylene groups, and oxidation potentials higher than those observed for aromatic oligothiophenes might be expected. This is not actually the case for H4Th4CN4, for which the first oxidation process occurs at a voltage lower than those reported for aromatic quaterthiophenes (0.95–1.05 V)²⁴ and similar to those observed for longer oligomers such as sexithiophenes (0.80–0.90 V).^{24,25} The voltage difference between the two oxidation processes is greater for H4Th4CN4 ($\Delta E = 0.54$ V) than for aromatic quaterthiophene (0.30–0.35 V) or sexithiophene (0.15–0.20 V), indicating the destabilization of the second positive charge for H4Th4CN4.

The appearance of reversible reduction and oxidation processes on the same oligothiophene chain is a novel observation in these molecular materials and reveals their ability to act as electron donors and electron acceptors in a large range of potential values.

Structure Calculations on Charged Species. To gain a deeper insight into the reduction and oxidation processes, the molecular geometries of the radical anion, dianion, radical cation, and dication of H3Th3CN4 and H4Th4CN4 were optimized at the B3LYP/6-31G** level (UB3LYP/6-31G** for open-shell radicals). To simplify the calculations, the hexyl chains were replaced by methyl groups and, in a first approach, all species were considered to be planar and all-anti (trimer, C_s ; tetramer, C_{2h}). Table 1 summarizes the B3LYP/6-31G**-optimized bond lengths calculated for the different redox states of the tetramer including the neutral molecule. Figure 5 sketches how the bonds constituting the CC conjugation path evolve with the redox state. Table 2 lists the net charges calculated for the different structural units of the tetramer.

- (24) (a) Guay, J.; Kasai, P.; Díaz, A.; Wu, R.; Tour, J. M.; Dao, L. H. *Chem. Mater.* **1992**, *4*, 1097. (b) Bäuerle, P.; Segelbacher, U.; Gaudl, K.-U.; Huttenlocher, D.; Mehring, M. *Angew. Chem., Int. Ed. Engl.* **1993**, *32*, 76. (c) Bäuerle, P.; Fischer, T.; Bidlingmeier, B.; Stabel, A.; Rabe, J. P. *Angew. Chem., Int. Ed. Engl.* **1995**, *34*, 303. (d) Casado, J.; Miller, L. L.; Pappenfus, T. M.; Mann, K. R.; Hernández, V.; López Navarrete, J. T. *J. Phys. Chem. B* **2002**, *106*, 3597.
- (25) Van Haare, J. A. E. H.; Havinga, E. E.; van Dongen, J. L. J.; Janssen, R. A. J.; Cornil, J.; Brédas, J.-L. *Chem. Eur. J.* **1998**, *4*, 1509. Cornil, J.; Beljonne, D.; Calbert, J.-P.; Brédas, J.-L. *Adv. Mater.* **2001**, *13*, 1053.

Table 1. B3LYP/6-31G**-Optimized Bond Distances (Å) for R4Th4CN4 (R = CH₃, C_{2h} Symmetry) in Different Oxidation States



distance	neutral	anion	dianion	cation	dication
C1–C1'	1.388	1.416	1.438	1.412	1.438
C1–C2	1.416	1.394	1.378	1.404	1.395
C2–C3	1.375	1.399	1.419	1.388	1.398
C3–C4	1.449	1.420	1.400	1.436	1.430
C4–C5	1.392	1.419	1.442	1.409	1.417
C5–C6	1.448	1.419	1.399	1.447	1.457
C6–C7	1.373	1.394	1.414	1.377	1.372
C7–C8	1.423	1.404	1.388	1.420	1.426
C8–C9	1.390	1.413	1.437	1.390	1.381
C9–C10	1.423	1.417	1.411	1.424	1.425
C9–C11	1.422	1.415	1.410	1.423	1.425
C10–N1	1.166	1.169	1.173	1.165	1.164
C11–N2	1.166	1.169	1.173	1.165	1.164
S1–C1	1.763	1.759	1.759	1.747	1.735
S1–C4	1.783	1.781	1.782	1.773	1.771
S2–C5	1.788	1.787	1.789	1.770	1.753
S2–C8	1.752	1.751	1.755	1.753	1.760

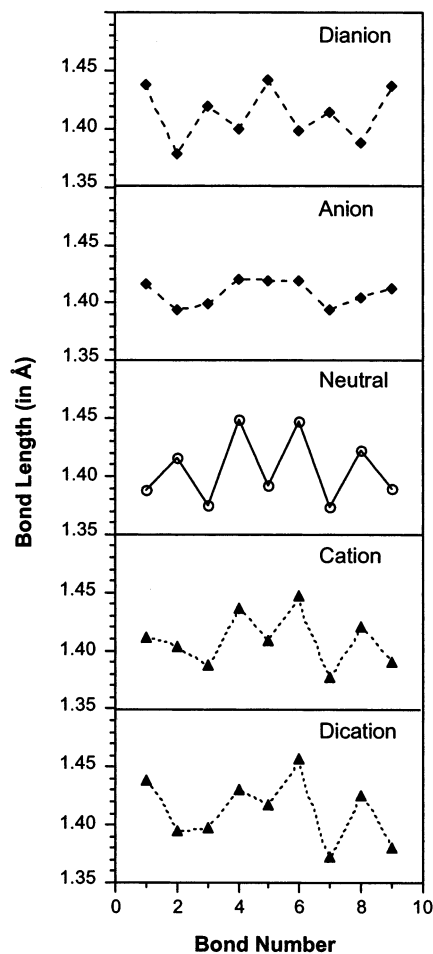
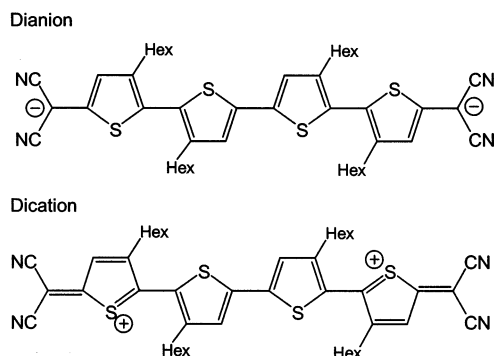


Figure 5. B3LYP/6-31G**-optimized bond lengths calculated for half the CC path of R4Th4CN4 (R = CH₃, C_{2h} symmetry). The bond numbering is from the center toward one end of the oligomer, bond number 1 corresponding to the central C1–C1' bond.

Reduction affects the whole oligothiophene backbone. In passing to the dianion, the inter-ring C1–C1' and C4–C5 bonds

Table 2. Mulliken Net Charges (e) Calculated at the B3LYP/6-31G** Level for R4Th4CN4 (R = CH₃, C_{2h} Symmetry) in Different Oxidation States

structural unit	neutral	anion	dianion	cation	dication
C(CN) ₂ group	-0.32	-0.50	-0.71	-0.11	+0.08
outer thiophene ring	+0.20	+0.02	-0.14	+0.35	+0.52
inner thiophene ring	+0.12	0.02	-0.15	+0.26	+0.39

Chart 1. Model Structures for the Dianion and Dication of H4Th4CN4

and the terminal C8–C9 bonds lengthen from 1.39 to 1.44 Å, thereby showing a single-bond character. The four thiophene rings undergo a reversal of the single–double CC bond alternation pattern, reaching an aromatic-like structure for the dianion as sketched in Chart 1.

The dicyanomethylene groups, which accumulate most of the charge introduced (–0.71e each), are slightly affected by reduction, showing a small lengthening of the C≡N bonds and a shortening of the C–CN bonds. These structural changes are easily understood by taking into account the topology of the LUMO (Figure 3), where the extra electrons are introduced. The LUMO spreads over the CC conjugation pathway with no contribution of the sulfur atoms and a negligible contribution of the cyano bonds. Similar structure changes are obtained for the trimer upon reduction.

Reduction thus causes the aromatization of the oligothiophene backbone. This aromatization together with the electron-withdrawing character of the C(CN)₂ justifies the stability of the reduced species. For the radical anion, the gain of aromaticity is only partial and its structure is intermediate between the quinonoid structure of the neutral molecule and that of the dianion (Table 1 and Figure 5). B3LYP/6-31G** calculations predict that the radical anions of the trimer and the tetramer are more stable than the respective neutral molecules by 3.19 and 3.27 eV (adiabatic electron affinities). Aromatization of the oligothiophene backbones is completed for the dianions, which are more stable than the neutral molecules by 3.30 eV (trimer) and 3.80 eV (tetramer). The dianions are therefore predicted to be more stable than the respective radical anions. Assuming that solvent effects do not alter this trend, this theoretical result explains the fact that only one two-electron reduction wave directly leading to the dianion is observed in the CVs of H3Th3CN4 and H4Th4CN4. This is not the case for the parent TCNQ, for which B3LYP/6-31G** calculations predict that the radical anion and the dianion are 3.35 and 2.35 eV more stable than the neutral molecule, respectively, and two well-separated one-electron reduction processes are experimentally observed.

We turn now to discuss the effects of oxidation on the molecular structure. As illustrated in Table 1 and Figure 5 for

the tetramer, the extraction of electrons mainly affects the central part of the molecule. In going to the dication, the C1–C1' bond lengthens to 1.44 Å, similar to that found for the dianion, the C4–C5 bonds lengthen slightly to 1.42 Å, and the C8–C9 bonds slightly shorten to 1.38 Å, preserving their double-bond character. The charging process slightly aromatizes the inner thiophene rings, but it affects neither the quinonoid structure of the outer rings nor the dicyanomethylene groups. These structural changes can be understood by looking at the topology of the HOMO (Figure 3), from which electrons are extracted. This orbital is mainly located on the central bithiophene unit and shows nonbonding contributions on the outer regions of the molecule.

The main structural effect of oxidation is therefore the slight aromatization of the inner thiophene rings. The structure sketched in Chart 1 for the dication shows this partial aromatization and emphasizes the fact that the dicyanomethylene groups are not involved in oxidation. However, the structure is not a faithful representation of the molecular geometry of the dication since no large difference is calculated between the C–S bond lengths (see Table 1) and the positive charge is almost equally shared among the sulfur atoms. The partial aromatization of the oligothiophene backbone contributes to the stabilization of the radical cation and dication species, thereby explaining the low oxidation potentials observed experimentally for H3Th3CN4 and H4Th4CN4.

The lengthening of the inter-ring bonds for both reduced and oxidized species opens the possibility of internal rotations around these bonds to avoid interannular steric interactions. We explored this possibility for both the dianion and the dication of the tetramer by reoptimizing their molecular geometries under no symmetry restriction. The dianion relaxes to a twisted structure in which the outer rings form a dihedral angle of 45° with the inner rings and the central bithiophene structure remains almost planar. The twisted structure is 1.24 kcal/mol (0.05 eV) more stable than the planar C_{2h} structure and contributes to the additional stabilization of the dianion. The dication converges to the planar C_{2h} structure due to the shorter length of the C4–C5 bonds (1.417 Å). On the basis of these results and the lengths of the inter-ring bonds found for the radical anion and radical cation (1.41–1.42 Å), planar structures have to be expected for these species.

Vis–Near-IR Spectra. Figure 6 shows the electronic absorption spectra recorded for H4Th4CN4 upon electrochemical reduction and oxidation. Table 3 summarizes the wavelengths measured for the absorption features of H4Th4CN4.

To investigate the electronic transitions that give rise to the absorption bands observed experimentally, the lowest-energy electronic excited states of both H3Th3CN4 and H4Th4CN4 in their different redox states were calculated at the B3LYP/6-31G** level using the TDDFT approach. Calculations were performed on the molecular models discussed in the previous section, for which hexyl chains are replaced by methyl groups. It will be seen that TDDFT calculations allow for a complete assignment of the optical features observed for H4Th4CN4 in neutral, reduced, and oxidized states.

The neutral species of H3Th3CN4 and H4Th4CN4 show an intense electronic band at 672 and 790 nm, respectively, with shoulders at 720 and 871 nm (assigned as vibronic structure) for the tetramer. These bands, which are reasonably expected

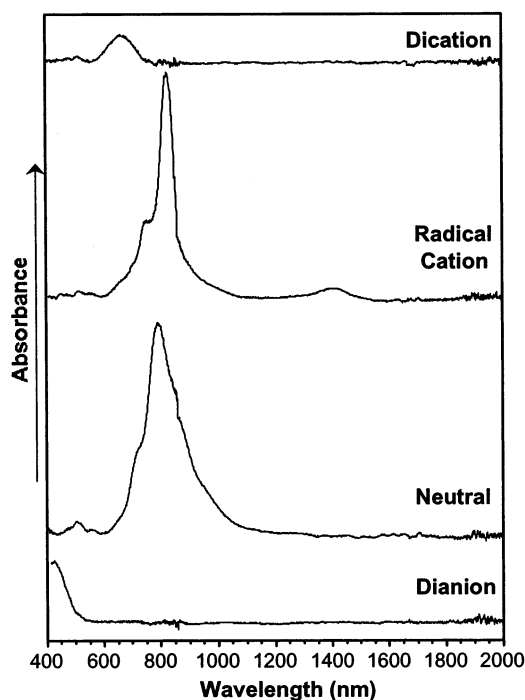


Figure 6. Vis-near-IR spectra recorded in CH_2Cl_2 solution during the electrochemical reduction and oxidation of H4Th4CN4 .

Table 3. Wavelength Maximum Values Measured for the Electronic Bands of Neutral and Reduced/Oxidized Species of H4Th4CN4

species	wavelength (nm)	species	wavelength (nm)
H4Th4CN4	720 (sh), 790, 871 (sh)	H4Th4CN4^+	748 (sh), 825, 1404 (w)
H4Th4CN4^{2-}	420	H4Th4CN4^{2+}	666

to originate in the $\pi-\pi^*$ transition of the oligothiophene backbone, are largely red-shifted with respect to the electronic absorptions that aromatic oligothiophenes present around 400 nm.^{24,28}

B3LYP/6-31G** calculations on the neutral molecules predict that the transition to the first excited electronic state, computed at 2.00 eV above the ground state for the trimer and at 1.68 eV for the tetramer, is dipole-allowed and shows a large value for the oscillator strength ($f = 1.77$ and 2.38, respectively). No other electronic transition with a significant intensity ($f \geq 0.1$) is calculated below 3.25 eV. The intense absorption bands observed at 672 nm (1.85 eV, trimer) and 790 nm (1.57 eV, tetramer) are therefore assigned to the transitions calculated at 2.00 and 1.68 eV, respectively, which correspond to one-electron HOMO \rightarrow LUMO excitations. The atomic orbital composition of these orbitals (Figure 3) reveals that these transitions mainly involve the oligothiophene backbone and that no intramolecular charge transfer to the dicyanomethylene groups is detected. The low energy of these transitions arises from the heteroquinonoid structures of the neutral molecules, which lead to very small HOMO-LUMO gaps. The energies are in fact similar to those observed for aromatic oligothiophenes in the dication or bipolaron state,^{24a,29,30} for which quinonoid structures are

predicted. For instance, the dication of an end-capped aromatic quaterthiophene exhibits an intense absorption band at 775 nm (1.60 eV),³⁰ very close to that measured for H4Th4CN4 (790 nm).

Spectroelectrochemical studies of H4Th4CN4 in 0.1 M TBABF₄/ CH_2Cl_2 solution lead to the observation of three different redox processes. Electrolysis at negative potentials causes the disappearance of the absorptions from the neutral molecule, and the appearance of a band at 420 nm (2.95 eV). This value is consistent with the existence of an aromatic oligothiophene backbone after the incorporation of two electrons per molecule and predicts that the dianion should have a spectrum similar to the spectra of neutral oligothiophenes. Indeed, wavelength values around 400 nm have been extensively reported for the main absorption band in aromatic oligothiophenes.²⁴⁻²⁸ The species involved in the neutral (quinonoid) \rightarrow dianion (aromatic) reduction process for H3Th3CN4 and H4Th4CN4 can therefore be identified, from both structural and electronic standpoints, with those participating in the dication (quinonoid) \rightarrow neutral (aromatic) process for oligothiophenes.

The TDDFT calculations performed for the dianion confirm the appearance of a new electronic transition at higher energies (trimer, 2.58 eV, $f = 0.95$; tetramer, 2.12 eV, $f = 1.69$; results for the more stable twisted structure) than for the neutral molecule. The calculated energies underestimate the experimental values. The new transition corresponds to an electronic excitation from the LUMO of the neutral molecule, which is doubly occupied for the dianion, to the LUMO+1.

Electrolysis of H4Th4CN4 at $E_{\text{app}} = +0.9$ V causes the appearance of an intense band at 825 nm (1.50 eV) with a shoulder at 748 nm (1.66 eV) and a weak band at 1404 nm (0.88 eV). Further oxidation at $E_{\text{app}} = +1.4$ V results in the decrease in intensity of the bands at 825 and 748 nm as a new band grows in at 666 nm (1.86 eV).

The electronic spectrum calculated for the cation radical assigns the band observed at 0.88 eV to the transition to the first excited state ($1^2\text{A}_u \rightarrow 1^2\text{B}_g$). This transition is calculated at 0.87 eV and has an oscillator strength $f = 0.10$ in agreement with the weak intensity observed experimentally. The transition is mainly described by a one-electron excitation from the singly occupied HOMO to the LUMO with an important contribution of the HOMO-1 \rightarrow HOMO excitation. Calculations attribute the intense band at 1.50 eV to the transition to the second 2^2B_g excited state calculated at 1.71 eV. The transition is computed to have a large oscillator strength ($f = 2.05$) and mainly results from the HOMO-1 \rightarrow HOMO monoexcitation. Theoretical calculations also suggest that the shoulder observed at 1.66 eV corresponds to a vibration component, since the next dipole-allowed transition is found at 2.29 eV.

For the dication, the transition to the first excited state ($1^1\text{A}_g \rightarrow 1^1\text{B}_u$) is calculated at 1.91 eV and has an oscillator strength of 2.31. The energy calculated for this transition agrees with that observed for the experimental absorption band (1.86 eV). The $1^1\text{A}_g \rightarrow 1^1\text{B}_u$ transition implies a one-electron excitation from the HOMO-1 to the HOMO, which is completely empty for the dication.

(26) (a) van Pham, C.; Burckhardt, A.; Shabana, R.; Cunningham, D. D.; Mark Jr., H. B.; Zimmer, H. *Phosphorus, Sulfur Silicon Relat. Elem.* **1989**, *46*, 153. (b) Bäuerle, P. *Adv. Mater.* **1992**, *4*, 102.

(27) Hernández, V.; Hotta, S.; López Navarrete, J. T. *J. Chem. Phys.* **1998**, *109*, 2543.

(28) Hotta, S.; Waragai, K. *J. Phys. Chem.* **1993**, *97*, 7427.

(29) Hill, M. G.; Penneau, J.-F.; Zinger, B.; Mann, K. R.; Miller, L. L. *Chem. Mater.* **1992**, *4*, 1106.

(30) Bäuerle, P.; Segelbacher, U.; Maier, A.; Mehring, M. *J. Am. Chem. Soc.* **1993**, *115*, 10217.

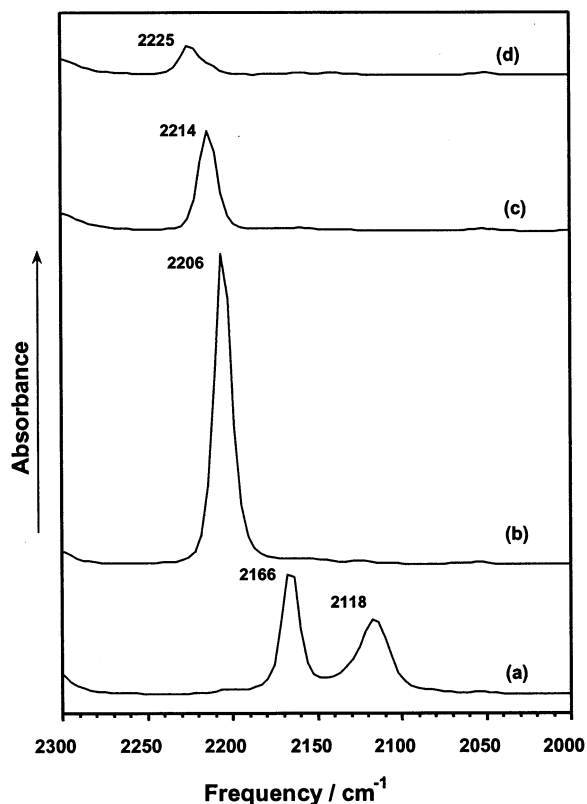


Figure 7. FT-IR spectra in the CN stretching region recorded in CH_2Cl_2 solution during the electrochemical reduction and oxidation of H4Th4CN4 : (a) reduced molecule, (b) neutral molecule, (c) first oxidized species, and (d) second oxidized species.

Infrared Spectroelectrochemical Results. Spectral changes in the IR region of the various redox states complement those seen in the UV-vis-near-IR region. Figures 7 and 8 show the infrared spectra of H4Th4CN4 recorded upon electrochemical reduction and oxidation.

Theoretical IR spectra were calculated at the B3LYP/6-31G** level for methyl-substituted models of H3Th3CN4 and H4Th4CN4 in both neutral and oxidized/reduced states. IR calculations were performed on the planar geometries previously optimized for the trimer (C_s) and the tetramer (C_{2h}). The IR spectrum of the dianion of the tetramer was also computed for the most stable twisted C_2 structure.

Infrared spectroscopy in the $\text{C}\equiv\text{N}$ stretching frequency region, $\nu(\text{CN})$, is useful for estimating the degree of intramolecular charge transfer (CT), since $\nu(\text{CN})$ is highly influenced by the redox state of the molecule. The IR peak corresponding to the CN stretching is observed at $2225 \pm 5 \text{ cm}^{-1}$ for neutral TCNQ .³¹ The $\nu(\text{CN})$ frequency downshifts as the TCNQ molecule is reduced and appears at 2197 cm^{-1} for TCNQ^- and at 2164 cm^{-1} for TCNQ^{2-} .³²

The $\nu(\text{CN})$ vibration is observed as a single-peak, medium-intensity band at 2211 cm^{-1} for H3Th3CN4 and at 2206 cm^{-1} for H4Th4CN4 . It was measured at 2214 cm^{-1} for the unsubstituted dimer Th2CN4 .^{2b} The frequency downshift as the size of the oligomer increases results both from the charge

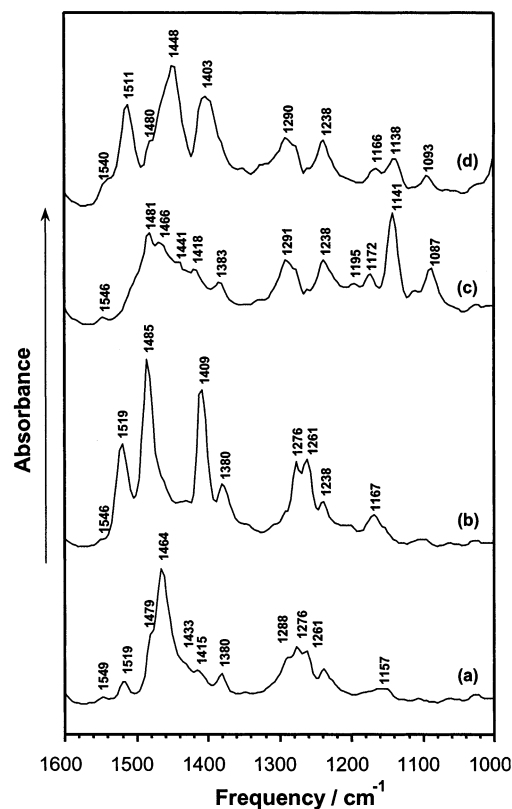


Figure 8. FT-IR spectra over probe energies of $1600\text{--}1000 \text{ cm}^{-1}$ recorded in CH_2Cl_2 solution during the electrochemical reduction and oxidation of H4Th4CN4 : (a) reduced molecule, (b) neutral molecule, (c) first oxidized species, and (d) second oxidized species.

transfer from the oligothiophene backbone to the $\text{C}(\text{CN})_2$ groups and from the greater extension of the conjugation path in which the $\text{C}(\text{CN})_2$ groups are involved. B3LYP/6-31G** calculations predict a similar downshift for the $\nu(\text{CN})$ frequency from the trimer (2238 cm^{-1}) to the tetramer (2235 cm^{-1}). For the tetramer, the frequency corresponds to a B_u normal mode in which the two CN bonds of each $\text{C}(\text{CN})_2$ group vibrate in-phase. The B_u normal mode in which the CN bonds vibrate out-of-phase is calculated at 2218 cm^{-1} but is not observed due to its small intensity (22:1 ratio).

After reduction of H4Th4CN4 , the CN stretching band splits into a doublet at 2166 and 2118 cm^{-1} . By comparison with TCNQ , these frequency values are consistent with the existence of a dianion charged species. The splitting of the CN band is also observed for TCNQ^{2-} , for which the double peak appears at 2164 and 2096 cm^{-1} .³² Theoretical calculations on the dianion of H4Th4CN4 reveal that the splitting of the CN frequencies is not due to a distortion of the molecular symmetry but is an inherent property of the isolated dianion. When the planar C_{2h} structure is used to calculate the IR spectrum, two CN active modes are found at 2190 and 2158 cm^{-1} with an intensity ratio of 3.5:1. The two modes correspond to those calculated for the neutral molecule, but now the out-of-phase mode has gained intensity. When the more stable twisted C_2 structure is used in the calculation, the doublet appears at the same frequencies with an intensity ratio of 2.1:1.

The CN stretching band of the H4Th4CN4 cation radical formed by electrolysis at $+0.9 \text{ V}$ is measured as a single peak at 2214 cm^{-1} shifted up from 2206 cm^{-1} for the neutral molecule. Extraction of the second electron shifts the peak to

(31) (a) Takenaka, T. *Spectrochim. Acta*, A **1971**, *27*, 1735. (b) Girlando, A.; Pecile, C. *Spectrochim. Acta*, A **1973**, *29*, 1859. (c) Faulques, E.; Leblanc, A.; Molini, P.; Decoster, M.; Conan, F.; Guerschais, J. E.; Sala-Pala, J. *Spectrochim. Acta*, A **1995**, *51*, 805.

(32) Khatkale, M. S.; Devlin, J. P. *J. Chem. Phys.* **1979**, *70*, 1851.

even higher frequencies at 2225 cm^{-1} with a shoulder around 2215 cm^{-1} . These values demonstrate that although the oxidation is centered on the thiophene rings, the CN groups are also affected. Mulliken population analysis supports this hypothesis since the net charge accumulated by each CN bond evolves from $-0.20e$ in the neutral molecule to $-0.13e$ in the cation and to $-0.05e$ in the dication. For the cation, UB3LYP/6-31G** calculations predict the CN active modes at 2233 and 2215 cm^{-1} with an intensity ratio of 7:1 in agreement with the single-peak band observed experimentally. For the dication, the CN active modes are calculated at higher frequencies (2247 and 2233 cm^{-1}), in accord with experiment, and have an intensity ratio of 2.7:1. This ratio justifies the shoulder observed at low frequencies in the experimental spectrum.

The analysis of the $1600\text{--}1000\text{ cm}^{-1}$ frequency region gives us information about the structural modifications on the oligothiophene backbone. The IR spectrum of H4Th4CN4 in dichloromethane solution shows the most intense band at 1485 cm^{-1} with strong bands at 1519 and 1409 cm^{-1} . These frequencies are similar to those observed in the solid state (1484 , 1523 , and 1408 cm^{-1} , respectively), where the most intense band corresponds to the 1408 cm^{-1} band.³³ Theoretical calculations predict three intense vibrations in this region at 1526 , 1484 , and 1422 cm^{-1} , the strongest band corresponding to the last one. The theoretical frequencies are in very good agreement with the observed values and allow for a one-to-one assignment of the experimental bands.

Figure 9 sketches the eigenvectors (atomic vibrational displacements) calculated for the normal modes associated with the three intense vibrations.

All three modes describe out-of-phase stretching vibrations of the CC double bonds. The mode calculated at 1526 cm^{-1} mainly involves the $C_{\beta}=C_{\beta}$ bonds of the outer thiophene rings. The mode at 1484 cm^{-1} mainly implies the $C_{\alpha}=C_{sp^2}$ bonds connecting the outer thiophene rings to the dicyanomethylene groups. The mode at 1422 cm^{-1} mostly corresponds to the movement of the $C_{\alpha}=C_{\alpha}$ bonds connecting the inner thiophene rings to the outer thiophene rings. There is actually a fourth mode calculated at 1535 cm^{-1} with a low intensity that can be correlated with the small band observed at 1546 cm^{-1} and that describes the out-of-phase stretching of the $C_{\beta}=C_{\beta}$ bonds of the inner rings.

The infrared spectrum of reduced H4Th4CN4 shows the most intense band at 1464 cm^{-1} and a medium–weak-intensity band at 1519 cm^{-1} . On the basis of the theoretical calculations performed for the dianion in its more stable twisted C_2 structure, the band at 1519 cm^{-1} corresponds to the out-of-phase anti-symmetric stretching of the $C_{\alpha}=C_{\beta}$ bonds [$\nu_{as}(C_{\alpha}=C_{\beta})$], which have double-bond character for the dianion. The normal mode involved in the most intense band describes the symmetric stretching of the $C_{\alpha}=C_{\beta}$ bonds [$\nu_s(C_{\alpha}=C_{\beta})$]. These vibrational normal modes are characteristic of aromatic oligothiophenes. The IR bands measured for reduced H4Th4CN4 appear in fact at frequencies similar to those observed for α,α' -dimethylquaterthiophene in CH_2Cl_2 solution (1521 and 1447 cm^{-1}).³⁴ These results confirm the aromatic structure predicted for H4Th4CN4 in the reduced or dianion state.

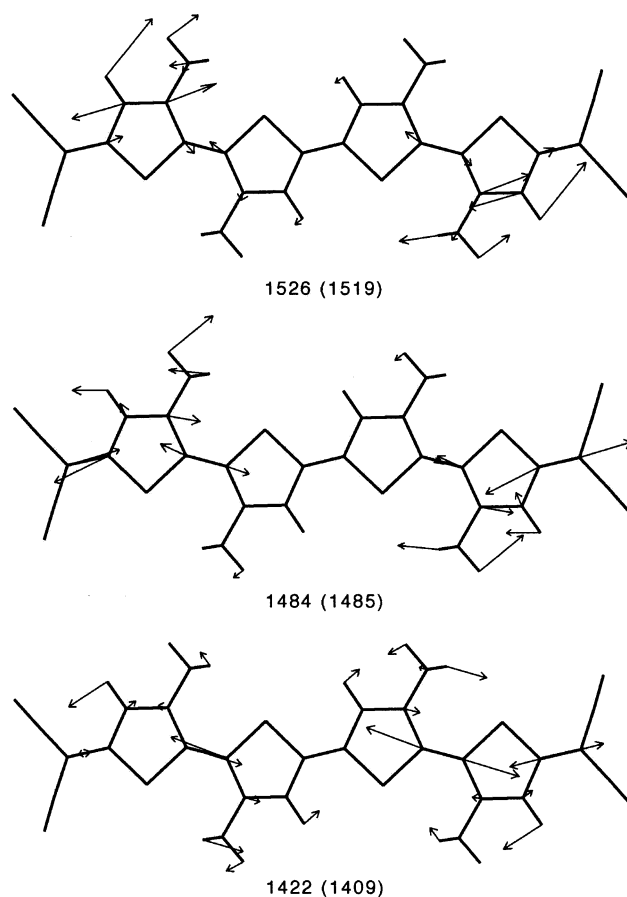


Figure 9. Schematic eigenvectors calculated at the B3LYP/6-31G** level for the most intense IR-active vibrations of R4Th4CN4 (R = CH₃). Scaled and experimental (within parentheses) wavenumbers are given in inverse centimeters.

The infrared spectrum of H4Th4CN4 oxidized at $+0.9\text{ V}$ shows a broad band in the $1500\text{--}1400\text{ cm}^{-1}$ region with a poorly resolved peak structure. When the molecule is oxidized at $+1.4\text{ V}$, the most intense band is observed at 1448 cm^{-1} and is flanked by two intense bands at 1511 and 1403 cm^{-1} . The peak features observed in the spectrum of the highly oxidized species are a mixture of those recorded for the neutral molecule (quinonoid) and for the dianion (aromatic). On one hand, the peaks at 1511 and 1403 cm^{-1} can be correlated with the peaks at 1519 and 1409 cm^{-1} of the neutral molecule. These peaks were associated with the stretching of the $\text{C}=\text{C}$ double bonds of the outer thiophene rings (see Figure 9), and these rings preserve its quinonoid structure for the dication (see Table 1). On the other hand, the central peak at 1448 cm^{-1} correlates with the most intense peak of the dianion at 1464 cm^{-1} . This peak was assigned to the symmetric $\text{C}=\text{C}$ stretching of the aromatic structure and here corresponds to the stretching of the CC bonds of the inner thiophene rings, which have a structure halfway between that of an aromatic ring and that of a quinonoid ring (see Table 1 and Figure 5). The evolution of the IR spectrum upon oxidation is thus consistent with the evolution of the structure of the oligothiophene backbone predicted by the theoretical calculations.

(33) Hernández, V.; Casado, J.; Higuchi, H.; Viruela, R.; Pou-Américo, R.; Ortí, E.; López Navarrete, J. T. To be submitted for publication.

(34) (a) Hernández, V.; Casado, J.; Ramírez, F. J.; Alemany, L. J.; Hotta, S.; López Navarrete, J. T. *J. Phys. Chem.* **1996**, *100*, 289. (b) Hernández, V.; Casado, J.; Ramírez, F. J.; Zotti, G.; Hotta, S.; López Navarrete, J. T. *J. Chem. Phys.* **1996**, *104*, 9271.

Conclusions

The quinonoid bis(dicyanomethylene)terthiophene H3Th3CN4 and -quaterthiophene H4Th4CN4 have been investigated using spectroelectrochemical experiments and DFT theoretical calculations. The oligothiophene backbones of the neutral molecules are calculated to have a heteroquinonoid structure similar to that predicted for aromatic oligothiophenes in the dicationic state. This heteroquinonoid structure is characterized by a strong absorption band in the red or near-infrared region. In the IR spectrum, the stretching vibrations of the CC double bonds are also consistent with a quinonoid structure. H3Th3CN4 and H4Th4CN4 can be viewed as structural and electronic analogues of two-electron-oxidized oligothiophenes.

Cyclic voltammetry results show that H3Th3CN4 and H4Th4CN4 exhibit a dual electrochemical behavior. On one hand, they are easily reduced to the dianion due to the presence of the electron-withdrawing dicyanomethylene groups and the aromatization of the oligothiophene backbone. The dianion is predicted to be more stable than the radical anion. On the other hand, they are oxidized to the cation and even to the dication at unexpectedly low potentials. H3Th3CN4 and H4Th4CN4 can, therefore, act as both electron-acceptor and electron-donor systems. This behavior makes these molecules especially attractive for technological applications since they might act as n-type or p-type semiconductors.

H3Th3CN4 and H4Th4CN4 also present an interesting electrochromism. Upon reduction to the dianion, the oligothiophene backbone becomes fully aromatized and H3Th3CN4 and H4Th4CN4 absorb around 400 nm similar to aromatic oligothiophenes in the neutral state. Upon oxidation the cation radicals absorb in the near-infrared region and the dications in the visible region. These spectra as well as the IR spectra have been assigned on the basis of DFT calculations.

The evolution of the IR spectra with the redox state also gives evidence of the evolution from a quinonoid structure to an aromatic structure upon reduction. The oxidized species show vibrational bands associated with quinonoid thiophenes, but they also present bands that give evidence of the transition to a partially aromatized structure.

Acknowledgment. The present work was supported by the Ministerio de Ciencia y Tecnología of Spain through the research projects BQU2000-1156 and PB98-1447. The group at the University of Málaga is indebted to the Junta de Andalucía for funding (Grant FQM-0159). The group at the University of Valencia acknowledges the Generalitat Valenciana for a grant (GR01-145). J.C. is grateful to the Ministerio de Educación y Cultura of Spain for a postdoctoral fellowship (Grant PF00-25327895). K.R.M. acknowledges the National Science Foundation for support under Grant CHE-9307837.

JA027161I